Effect of Silicon Compounds on Stress Corrosion Cracking of Alloy 600 in Caustic Solutions

M. Navas, D. Gómez-Briceño, M. García-Mazario,* and A.R. McIlree**

ABSTRACT

Silicon compounds are abundant in both steam generator tube deposits removed from operating plants and in the hide-out return analyses performed during plant operation. Despite their abundance, the effect of these compounds on the susceptibility to intergranular attack (IGA) and stress corrosion cracking (SCC) of alloy 600 (UNS N06600) has not been established clearly in laboratory tests or under operating conditions. The present work studied the effect of different compounds of silicon, such as silica (SiO₂) and sodium metasilicate (Na₂SiO₃), on the susceptibility to IGA/ SCC of alloy 600 in caustic solutions, with and without impurities. Experimental work included measurement of potentiodynamic polarization curves and development of stress corrosion tests with potentiostatic control at 315°C. Results of both tests indicated an inhibiting effect of silicon compounds on stress corrosion of mill-annealed (MA) alloy 600. Polarization curves in solutions with silicon compounds showed a wider range of passivation and a reduction in passive current density and anodic dissolution compared to the curves obtained in sodium hydroxide (NaOH). In corrosion tests performed in solutions containing silicon compounds, cracking appeared at only some of the potentials tested and with much reduced depth. Judging by the results obtained from analyses of the surface deposits, the inhibiting effect appeared to be related to the incorporation of silicon in the oxide layer. Regarding the effect of impurities, these have been observed not to be harmful for the response of alloy

600MA to IGA/SCC, and would appear even to improve this response in solutions containing silicon compounds, probably caused by the formation of insoluble silicates.

KEY WORDS: alloy 600, Auger electron spectroscopy, caustic, intergranular attack, potentiodynamic polarization, potentiostatic, silicon, stress corrosion cracking, UNS N06600

INTRODUCTION

Intergranular stress corrosion cracking (IGSCC) and/ or intergranular attack (IGA) are the most frequently observed types of degradation in the steam generator tubes of pressurized water reactor (PWR)-type reactors in the support plate crevices and the rolling zone. Historically, the environment existing in the support plate crevices has been considered highly caustic, in accordance with the results of laboratory tests and thermodynamic calculations performed using codes such as the Electric Power Research Institute (EPRI)-developed MULTEQ† computer program. Nevertheless, the information obtained from the analyses of deposits on pulled tubes and the improvements made to the calculation codes, because of the consideration of new species such as silicates,[1] indicate that less caustic, and even acid, environments may occur in the crevices of the steam generator tubes.

Despite the abundance of silicon compounds in hideout returns and in the deposits of pulled tubes, their effect on the behavior of steam generator tube materials has never been considered adequately. The information available is contradictory, and it is possible to encounter in the literature old results that

TABLE 1
Chemical Composition of Alloy 600MA (Heat Treatment 927°C, 4 min)

Heat	C	Mn	S	Si	Cr	Ni	Fe	Cu
96834L	0.038	0.27	0.001	0.30	15.88	74.83	8.2	0.01

indicate an inhibiting or an aggressive effect of silicon compounds in caustic environments. Differences in behavior may be associated with the type of silicon compound used in the tests. In general, silicates showed an inhibiting effect in tests performed with C-ring specimens[2-3] and capsules,[4] except in the case of highly concentrated solutions of sodium metasilicate (Na_2SiO_3).[5] Silica (SiO_2) showed an aggressive effect in solution with 50% sodium hydroxide (NaOH),[6-7] with the exception of the tests carried out by Airey using 10% NaOH.[8] Recently, certain authors have indicated that the degradation of alloy 600 (UNS N06600)[(1)] by IGA/SCC may be related to the formation of aluminium-silicate gels associated with nonprotective, chromium-rich oxide layers.[9] However, in the analyses performed on steam generator tube deposits from operating plants, it is possible to find high concentrations of silicates and aluminium-silicates in tubes affected by IGA[10-11] and in tubes without any kind of degradation.[12]

Lack of understanding of the role played by silicon compounds may be caused by the complexity of their chemistry,[13] which complicates laboratory testing and interpretation of the analyses of the deposits. High concentrations of SiO_2 in the crevices may react with the NaOH forming different polymerized species of sodium silicates that show retrograde solubility at the operating temperature of steam generators, which, in turn, precipitate, leaving free SiO_2 and/or NaOH in the solution.

The present work presented part of a research project and studied the effect of different silicon compounds, in particular SiO_2 and Na_2SiO_3, on the susceptibility of steam generator tube materials to IGA/SCC in caustic solutions, with and without impurities. Although the scope of the project included study of the behavior of alloy 600MA, thermally treated (TT) alloy 690 (UNS N06690), and shot-peening (SP) alloy 800 (UNS N08800), this article presents only the work performed on alloy 600MA.

EXPERIMENTAL

Tests were performed on alloy 600MA tubes measuring 3/4 in. (19 mm) in diameter, the chemical composition of which is shown in Table 1.

Tests were carried out in caustic solutions with additions of SiO_2 and Na_2SiO_3. In accordance with

the phase diagram for SiO_2/sodium oxide (Na_2O)/H_2O,[13] both test solutions were chosen such that the SiO_2/NaOH ratios were equal to 1, and the concentration of SiO_2 in the reference solution (10% NaOH) was as high as possible with all the remaining SiO_2 dissolved. Consequently, the test solutions were as follows:

— Reference solution: 10% NaOH;

— Reference solution plus 7.5% SiO_2 added as amorphous silica; and

— 15% solution of Na_2SiO_3 (which dissolved corresponding to 10% NaOH + 7.5% SiO_2).

To study the effect of typical chemical species in steam generator crevices, and taking into account the hideout return results from various operating plants, tests were performed using the aforementioned solutions with 0.8 g/L Cl^-, 0.3 g/L Mg^{2+}, 14 g/L $SO_4^=$, and 5.8 g/L Ca^{2+} (added as magnesium chloride [$MgCl_2$] and calcium sulfate [$CaSO_4$]).

Experimental work included the measurement of potentiodynamic polarization curves and the development of stress corrosion tests with potentiostatic control at 315°C. C-ring specimens with 2% deformation, isolated through the use of pieces of oxidized zircaloy, were used in both types of tests, performed in static nickel autoclaves with a capacity of 8 L. A cover gas of 5% hydrogen/95% argon was used in all tests to allow the use of the nickel reference electrode as a hydrogen electrode.

Polarization curves were performed at a sweep rate of 0.16 mV/s, using stressed C-ring specimens. A nickel rod and the nickel body of the autoclave were used as the reference electrode and counter electrode, respectively. Three polarization curves were obtained for each material-solution pair and were used as a basis for selecting the four values of the potential for subsequent SCC tests: corrosion potential (E_{corr}); active potential (E_{act}) prior to the initiation of passivation; anodic peak potential (E_{peak}); and passivation potential (E_{pass}).

During the SCC tests, 36 samples were tested simultaneously in each of the solutions, 12 of each of the materials tested (alloys 600MA, 690TT, and 800SP). Samples were distributed in four series of the nine specimens, 3 of each of the materials. One of the four potentials defined above was applied to each series of specimens. Tests were performed using a system capable of simultaneously applying a different potential to each of the series of specimens, and it was possible to record the current intensity of the specimens of each alloy as though an independent

---

(1) UNS numbers are listed in *Metals and Alloys in the Unified Numbering System*, published by the Society of Automotive Engineers (SAE) and cosponsored by ASTM.
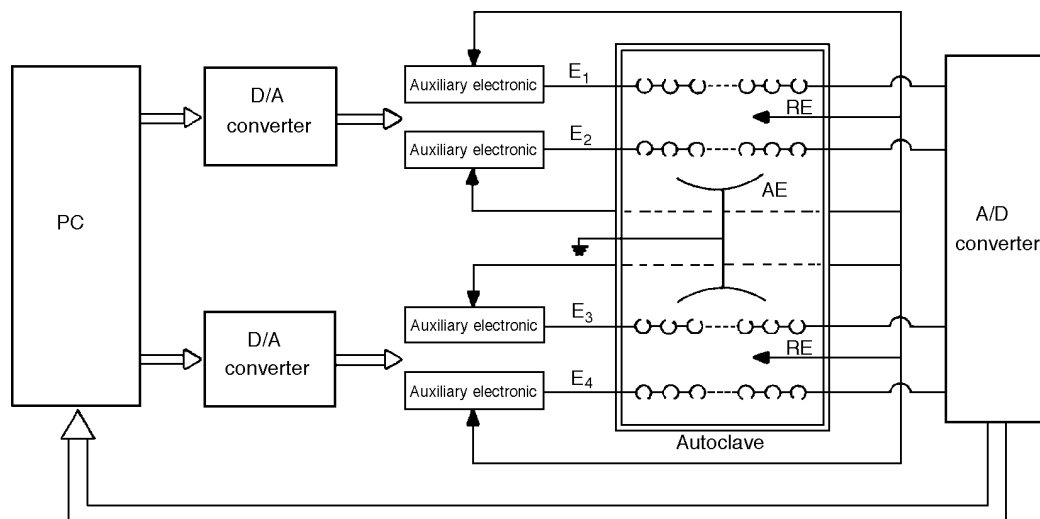
FIGURE 1. *Scheme of system used in multipotential corrosion tests (RE = nickel reference electrode; AE = auxiliary electrode, autoclave body; D/A = digital/analog; and A/D = analog/digital).*

potentiostat were used for each series. Figure 1 shows a diagram of the experimental device.

The total duration of the tests was 1,000 h, with two interruptions at 250 h and 500 h for the performance of visual inspections. Specimens that cracked during these inspections were removed and the rest continued the test with renewed solutions. On completion of the tests, a metallographic inspection was performed on all the cracked specimens to determine the maximum depth and morphology of the cracks. One of every three of the specimens, which had not revealed cracking during the visual inspection, was examined using metallographic techniques. If this specimen was found to be cracked, the other two also were examined.

In addition, the surface of the specimens was analyzed by means of Auger electron spectroscopy (AES) to determine the composition of the oxides and the concentration profiles of the deposit.

RESULTS

Potentiodynamic Polarization Curves

Figure 2 shows polarization curves obtained for alloy 600MA in the three solutions without impurities. Results indicated that the silicon compounds produced a significant change in the shape of the curves, with a wider passivation range and lower values of anodic peak and passivation current densities than those obtained in the reference solution. However, no significant differences were noted between the curves obtained in silicon compounds solutions, only the anodic peak current density was slightly lower with SiO_2 than in Na_2SiO_3.

Addition of impurities caused a reduction in current density and passivation potential, especially in

the case of the reference solution. Curves obtained in solutions with silicon compounds showed variations similar to those observed in solutions without impurities (Figure 3). The curve obtained with SiO_2 showed a lower current density and a slightly lower anodic peak potential.

Stress Corrosion Tests

The four values of applied potentials to the C-ring specimens in the corrosion tests are shown in Table 2. The final metallographic examination of some specimens showed cracks, which previously had not been observed during the visual inspection because of being covered with deposit, as was the case of the samples tested at E_{corr} in 10% NaOH, or to their small size, as was the case of the solutions with silicon compounds.

Results of these tests are shown in Figures 4 and 5 for solutions without and with impurities, respectively. These figures show the average value of maximum depth of the cracks detected in the three specimens, with the test time and applied potential. In both figures, the specimens tested in solutions containing silicon compounds showed greater resistance to SCC than those tested in the reference solution.

Caustic Solution — Alloy 600MA showed cracking in 10% NaOH at all potentials tested after 250 h, with the exception of E_{corr}, where cracking was detected by metallography after 750 h. During metallographic examination of the specimens, it was observed that the cracks were covered by a 100% nickel layer, according to energy dispersive spectroscopy (EDX) analysis. In Figure 6, the continuous layer of nickel covering the cracks can be seen. In certain cases, the material showed signs of cold-
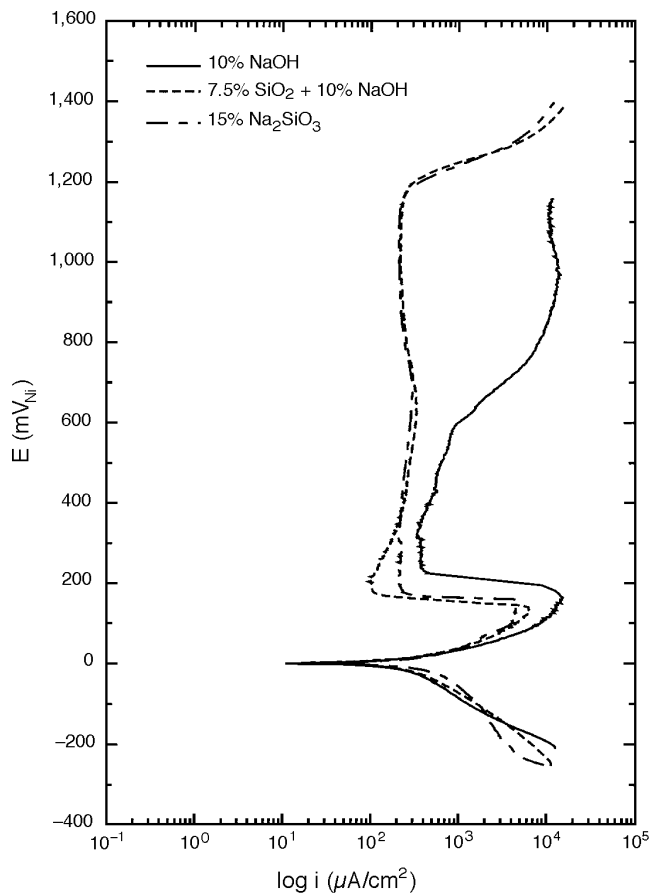
FIGURE 2. *Potentiodynamic polarization curves of alloy 600MA in different environments at 315°C.*
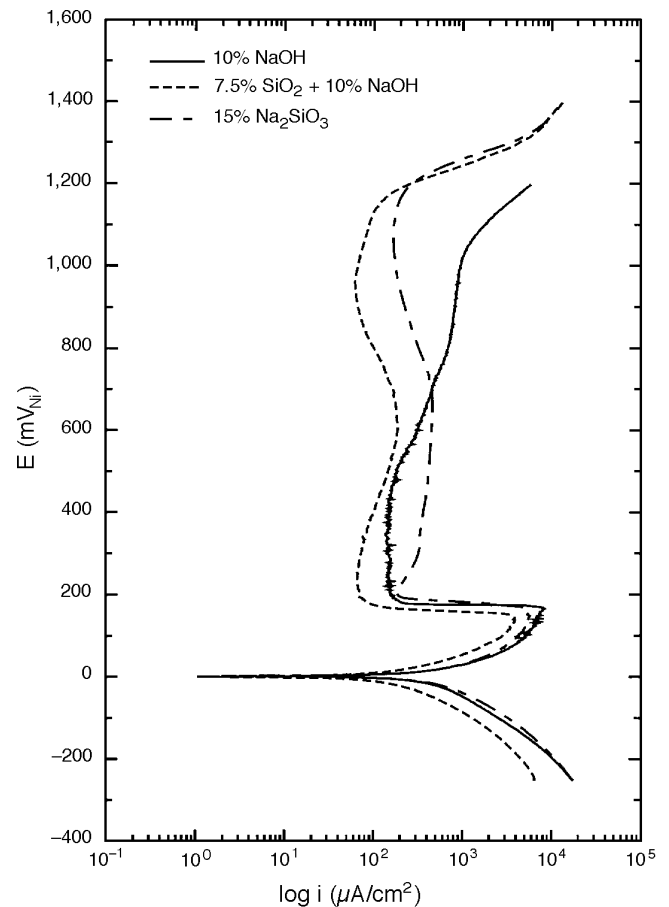
FIGURE 3. *Potentiodynamic polarization curves of alloy 600MA in different environments, plus impurities at 315°C.*

working beneath the layer of nickel, this indicating that this film had been deposited over the base material. The existence of this layer prevented the determination of crack formation time during the intermediate visual inspections. As the value of applied potential increased, the number of intergranular cracks decreased and maximum crack depth grew (Figures 7 and 8). However, it was not possible to establish a clear effect between applied potential and crack depth from these results.

In tests performed in caustic solution with impurities, samples tested at E_{corr} and E_{act} showed cracking after 1,000 h of testing, with smaller crack depths than in the reference solution. In both cases, intergranular cracking was associated with IGA at the grain edge (Figures 9 and 10). In specimens tested at E_{corr}, there was also a nickel layer, although this was not continuous as in the case of solutions without impurities. In specimens tested at E_{act}, there were, in addition to branched intergranular cracks, signs of material dissolution (Figure 10). At potentials E_{peak} and E_{pass}, unbranched cracks were observed with larger depths than in cases of two lower potentials and shorter times (Figure 11, 250 h).

Caustic Solutions with Silicon Compounds — Different types of deposits formed on the specimens tested in solutions containing silicon compounds with different colors and thicknesses depending on the potential. These deposits were especially adherent in the case of the two, more anodic potentials.

In the solution with pure SiO_2, the visual inspection performed after 250 h of testing revealed minor cracking only in the case of the specimens tested at E_{act} (Figure 12). After 1,000 h of testing, cracks also were detected at E_{peak} and slight penetrations at E_{pass}. Addition of impurities led to better behavior of alloy 600MA, since defects appeared at E_{act} only after 1,000 h of testing (Figure 13), and no cracking was detected at the other potentials.

In the case of the silicate solutions without impurities, cracks were observed at E_{act} only after 1,000 h of testing (Figure 14), their depth being similar to that obtained with solutions containing SiO_2. Addition of impurities did not modify the results obtained, as can be observed by comparing the cracks obtained at E_{act} in silicate solutions with and without impurities (Figures 14 and 15).

TABLE 2

Applied Potentials in Multipotential Potentiostatic Stress Corrosion Tests

Chemical Environment	E_{corr} (mV_{Ni})	E_{act} (mV_{Ni})	E_{peak} (mV_{Ni})	E_{pass} (mV_{Ni})
10% NaOH	2	100	150	200
7.5% SiO_2 + 10% NaOH	2	80	130	180
15% Na_2SiO_3	2	80	130	180
10% NaOH plus impurities	3	130	170	220
7.5% SiO_2 + 10% NaOH plus impurities	3	100	150	200
15% Na_2SiO_3 plus impurities	2	130	170	220
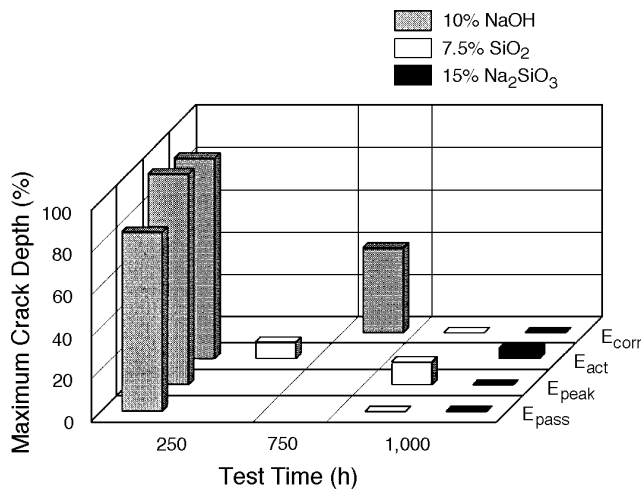
FIGURE 4. *Results of multipotential corrosion tests of alloy 600MA tested in different environments at 315°C.*
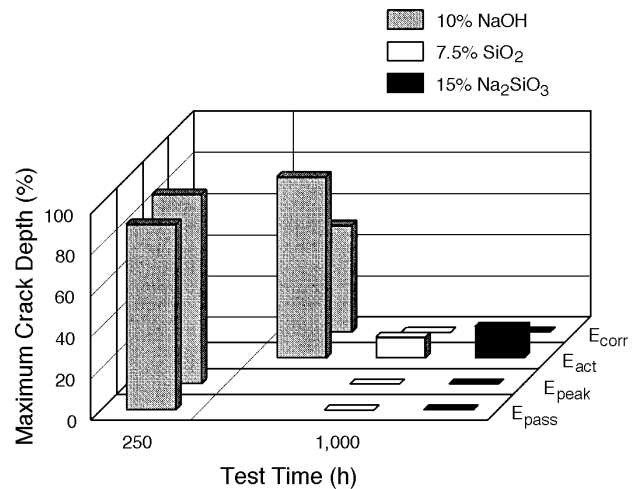
FIGURE 5. *Results of multipotential corrosion tests of alloy 600MA tested in different environments, plus impurities at 315°C.*

Results of Auger Analysis

Caustic Solution — The composition with depth of the oxide layers formed on the outer surface of the four specimens tested with 10% NaOH at different potentials was determined by AES. In the sample tested at E_{corr}, the absence of oxygen in the outer surface layer confirmed that the layer observed during the metallographic examination was of pure nickel (Figure 16). However, the oxide layer at the fracture surface was nickel-enriched with the presence of oxygen.

For the rest of the specimens, it was not possible to analyze the outermost surface because of charging problems, as a result of which the depth profiles were obtained where the layer had been broken or where it had been removed by handling. According to the literature, these problems arise because of the formation of a layer of chromium oxide.

Figure 17 shows that the oxide layer on the outer surface of a specimen tested for 250 h at E_{act} was made up of an inner layer showing nickel enrichment, similar to that found at the fracture surface of the E_{corr} specimen, and an outer layer enriched in chromium and iron. In the inner layer, the Ni/Cr ratio was greater than in the base material. In the

outer layer, this ratio was smaller than in the base material. Oxide layers on the specimens tested at potentials E_{peak} and E_{pass} were very similar and were formed by a single layer showing enrichment in chromium, like the outermost layer of the specimen tested at E_{act} (Figure 18).

Analyses performed on the outer surface of the specimens tested at E_{corr} and E_{pass} in 10% NaOH with impurities showed the same trend as those obtained in the reference solution (Figure 19). Of the impurities added, only calcium was incorporated into the deposits, the presence of sulfur, chlorine, or magnesium were not being detected.

Caustic Solutions with Silicon Compounds — Specimens tested in solutions containing silicon compounds were covered with abundant deposit, which caused charging problems in the Auger analyses. Consequently, analyses were performed on those specimens in which the thickness of the deposits was smaller or where such deposits were absent. Two specimens tested at E_{pass} were analyzed: one tested in SiO_2 solution and the other in Na_2SiO_3. In both cases, silicon had been incorporated into the oxide layers, and there were only minor differences regarding concentration in the outermost layer. Both specimens

showed weak nickel enrichment (Figure 20). In addition, in the case of the specimen tested in Na_2SiO_3, the sodium was incorporated through the entire thickness of the oxide layer; while in the specimen tested in SiO_2, it was not visible in the outermost layer.

To study the effect of the impurities, analyses were performed on specimens tested at E_{corr} and E_{pass} in the solution of Na_2SiO_3. As was the case in these solutions without impurities, only a slight enrichment in nickel occurred at E_{pass} (Figure 21). However, silicon, sodium, and magnesium also were seen to be incorporated into the layer. In the case of the specimen tested at E_{corr}, only silicon and sodium were incorporated into the outermost layer.

DISCUSSION

Caustic Solution

The shape of the polarization curves obtained in 10% NaOH was similar to those included in the literature,[14-16] although the anodic peak potential value was slightly higher. Differences in the experimental setup used by the authors, and the fact that in other works different types of specimens frequently are used to obtain polarization curves and to perform corrosion tests under potentiostatic control, may explain these differences. Usually, polarization curves are developed using small, flat, polished specimens. In SCC tests, stressed specimens are used, manufactured from as-received steam generator tubes.[15-16] In the present tests, stressed C-ring specimens were used for polarization curves and for SCC tests, since certain differences were observed in the curves obtained from stressed and nonstressed specimens. Furthermore, this methodology ensured the potentials applied during the corrosion tests were those selected from the polarization curves.

Effect of the applied potential on the susceptibility of alloy 600 to SCC, observed in short tests by other authors,[14-16] seemed to disappear when the testing time was sufficiently long, in spite of the different characteristics regarding the composition and thickness of the oxide layers formed. Surfaces of the specimens tested at E_{corr} were covered by a layer of pure nickel and not by a layer of oxide, as was to be expected given the presence of cracking. Nevertheless, at the crack fracture surfaces, the presence of oxygen was identified associated with the elements of the matrix. Indications of cold-working visible on the outer surface of the specimen ruled out the existence of a process of dealloying and indicated that the layer of nickel was deposited over the base material. The presence of cracking supported the idea of the protective characteristics of this layer being similar to those of the oxide layers required for crack formation. It is accepted that the presence of an oxide layer is necessary for the existence of IGSCC processes,
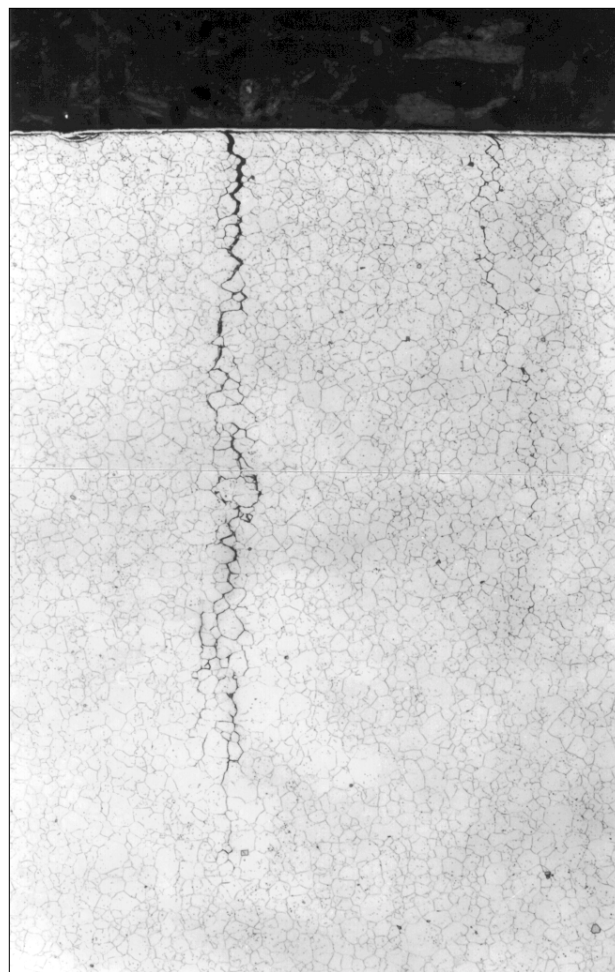

FIGURE 6. *Detail of specimen tested in 10% NaOH at E_{corr} during 750 h (200x).*

and at pH >10, the absence of the layer will give rise to IGA as long as the potential-pH conditions allow for slight dissolution of the nickel.[17-18] Formation of IGA is not likely in the presence of hydrogen because of the stability of the metallic nickel, this agreeing with the absence of IGA detected in the present tests.

Consequently, two different processes may have given rise to the formation of the layer of metallic nickel. It is possible the reduction of the different species of nickel dissolved in the test solution from the specimens tested at other potentials and the autoclave body or the reduction of the nickel oxide. The reduction of the dissolved nickel occurred only in those specimens whose applied potential was equal to E_{corr} and not in the rest of the specimens with more anodic potentials, where nickel oxide was the stable compound. This hypothesis was supported by the results obtained by Pinard-Legry and Plante,[2] who also found a thin layer of nickel on the surface of Fe-Cr-Ni alloy specimens tested in caustic environments at cathodic potentials, this suggesting the possibility of two cathodic reactions: the reduction of
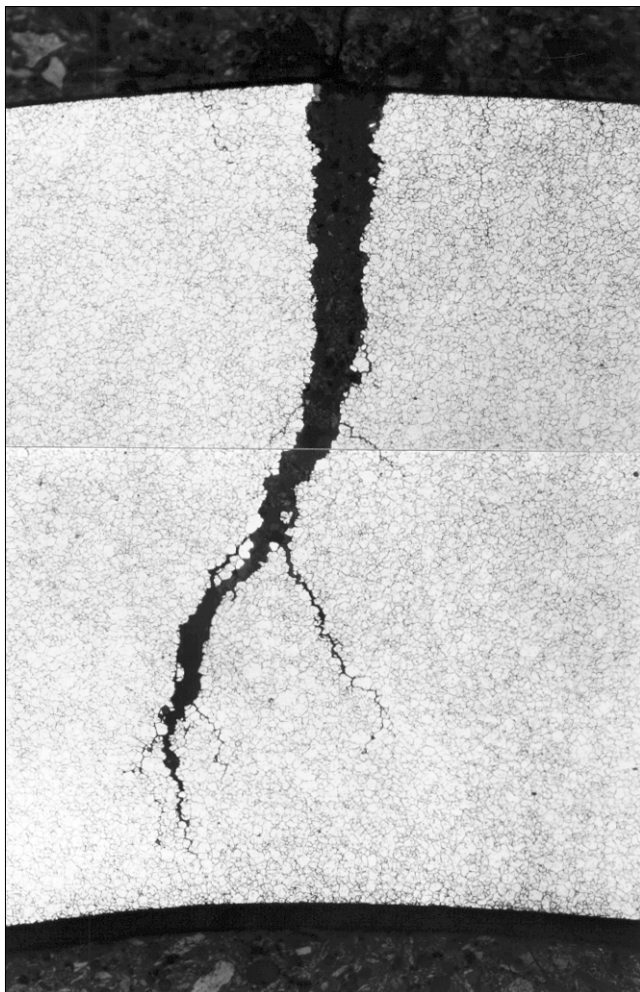
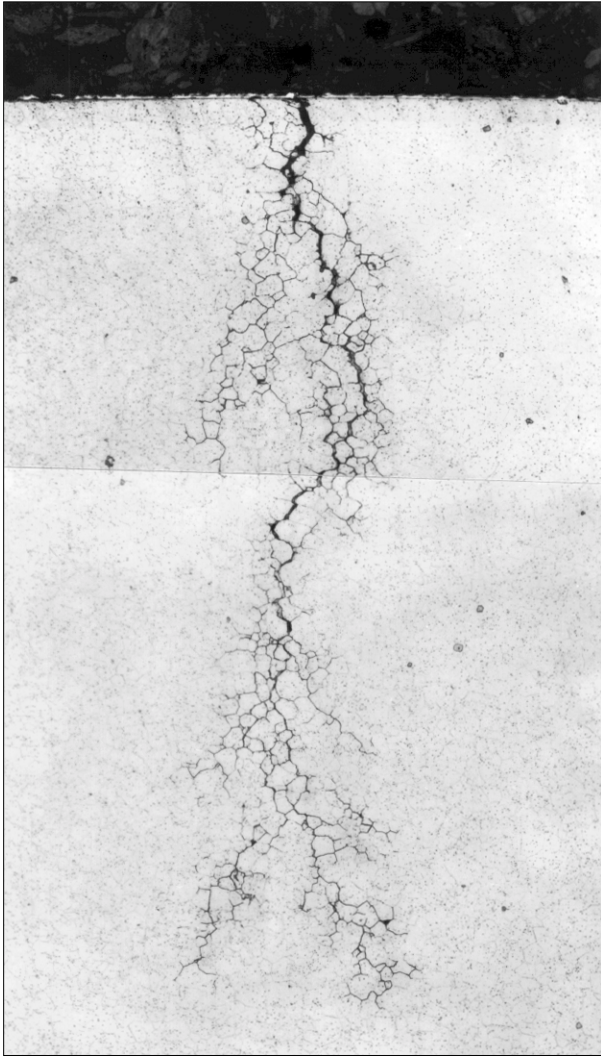**FIGURE 7.** *Alloy 600MA tested in 10% NaOH at E_{act} during 250 h (100x).*
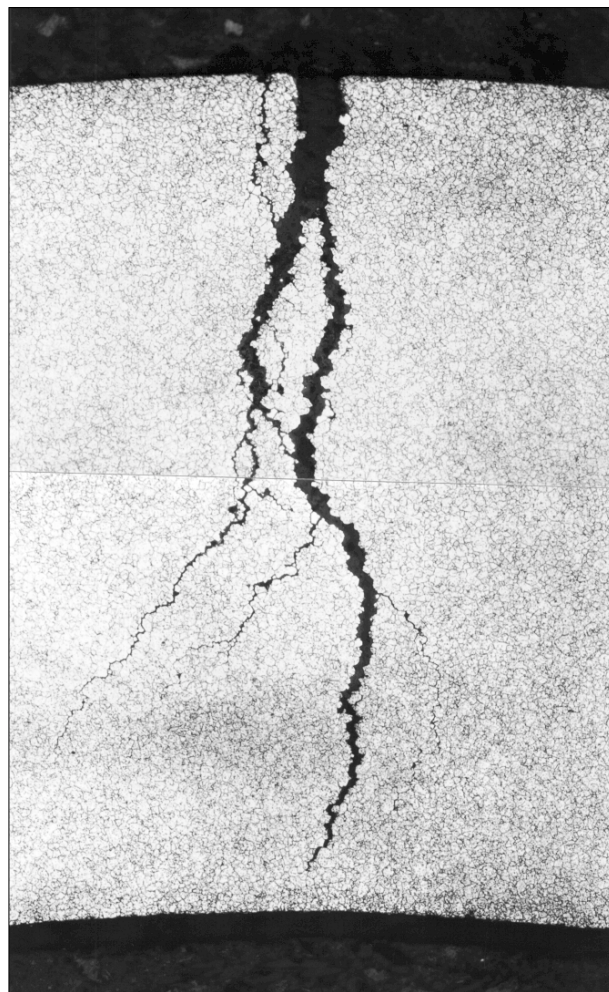
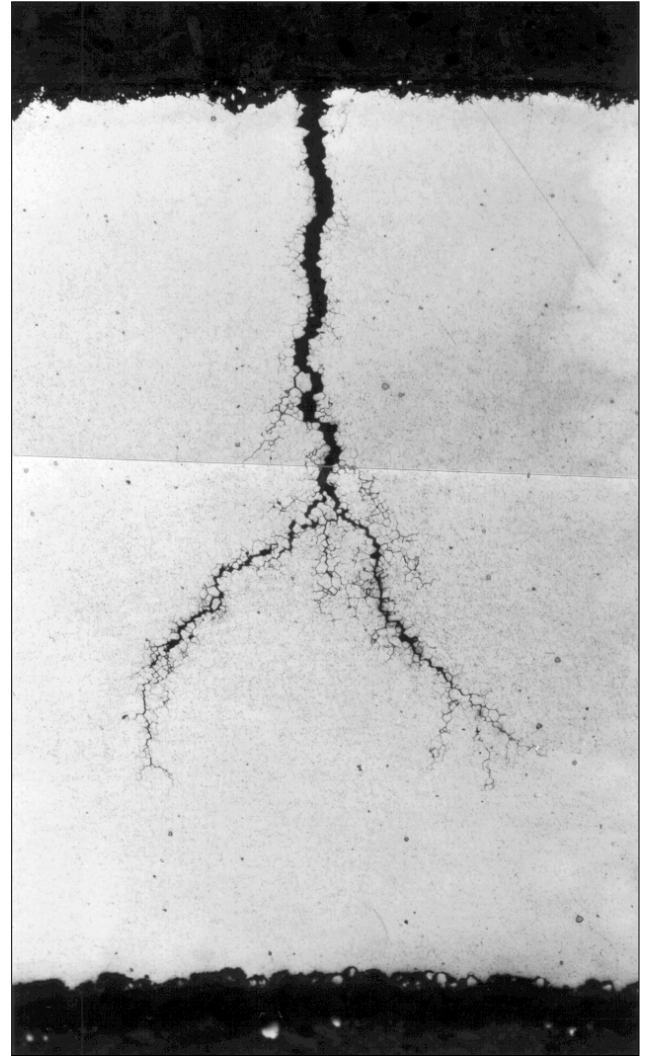**FIGURE 8.** *Alloy 600MA tested in 10% NaOH at E_{peak} during 250 h (100x).*

hydrogen and nickel. However, the nickel layer may have been the result of the reduction of oxides or hydroxides formed previously on the material, caused by increasing concentrations of hydrogen throughout the test.[19] This appeared to agree with results obtained from analysis of the surface, which indicated the presence of metallic nickel on the outer surface, and of nickel oxides and hydroxides at the fracture surface.

Results of the surface analyses indicated that the oxide layers formed at E_{peak} and E_{pass} showed a similar trend, with a smaller Ni/Cr ratio than in the base material, which appeared to contradict what was referred to in the literature as being representative of caustic environments. Nevertheless, the outermost layer of specimens tested at E_{act} showed a smaller Ni/Cr ratio than in the base material, but larger in the layer adjacent to it. To explain this unexpected behavior, an analysis was made of the records of evolution of current intensity acquired during the corrosion tests at each of the potentials.

At the three most anodic potentials, current intensity decreased from the initial value to a minimum value that appeared to correspond with the formation of a passive, nonprotective layer. The time required to reach this minimum value and the initial and minimum values of intensity depended on the applied potential. In the case of specimens tested at potentials E_{peak} and E_{pass}, the reduction of current intensity was very fast, as corresponding with the formation of the layer made up of nickel, chromium, and iron oxides and hydroxides, with depletion of nickel. At E_{act}, there was a process of material dissolution for 1 or 2 days, in which current intensity values remained high because of the preferential dissolution of metallic chromium. This gave rise to the formation of the nickel-enriched layer adjacent to the base material, prior to the formation of the outer layer with a Ni/Cr ratio lower than in the base material, similar to that found in the specimens tested at the other two more anodic potentials. Current intensities measured indicated that the application of potentials to the

FIGURE 9. *Detail of alloy 600MA tested in 10% NaOH, plus impurities at E_{corr} during 1,000 h (200x).*

FIGURE 10. *Alloy 600MA tested in 10% NaOH, plus impurities at E_{act} during 1,000 h (100x).*

specimens accelerated dissolution of the material, preferentially chromium, establishing a gradient of chromium concentration throughout the thickness of the oxide layer prior to the precipitation of the outer layer of chromium, iron, and nickel oxides and hydroxides, which were stable under the test conditions. Recent potential-pH diagrams showed the stability of chromium oxide in regions in which it was considered previously not to be stable.[20]

Under those conditions, in which the dissolution of the base material was small, as would be expected when the material was not polarized, the oxide layers were rich in nickel, as has been observed in the steam generator tubes from operating plants. If, however, the dissolution of the base material was favored, the preferential dissolution of chromium would have given rise to double oxide layers, with the outer layer enriched in chromium. Furthermore, taking into account that throughout most of the test specimens

tested at the three anodic potentials had low current densities and probably the same layers of oxides on the outermost surface, their response to SCC should have been similar over longer testing times.

Impurities added to the reference solution would appear not to have any harmful effect and may even mitigate the aggressiveness of caustic solutions. Polarization curves did not change in this environment, and only a slight reduction in current densities was observed. In general, the behavior of the material was similar at all the potentials tested, with the exception of the specimens tested with impurities at E_{act} where there was dissolution of the material in addition to SCC. According to results of oxide layer analysis, the possible beneficial effect of the impurities might have been caused by the incorporation of calcium. A similar effect has been observed in tests performed on steam generator model boiler,[21] where the addition of calcium hydroxide (Ca[OH]$_2$) changed the mode of
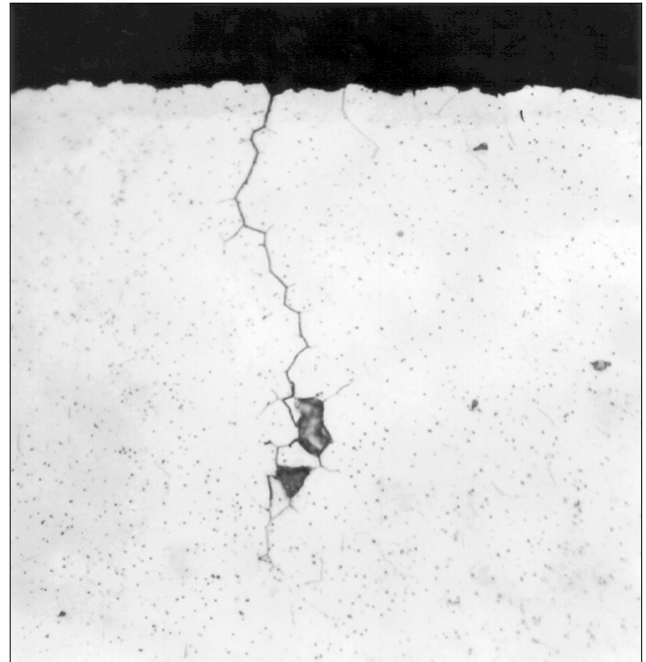
FIGURE 11. *Alloy 600MA tested in 10% NaOH, plus impurities at E_{peak} during 250 h (100x).*

FIGURE 12. *Detail of alloy 600MA tested in 7.5% SiO_2 + 10% NaOH at E_{act} during 250 h (500x).*

SCC attack to surface IGA in environments containing hydrazine and carbonates. This effect might have been caused by a change in the potential of the material or by a plugging mechanism preventing contact between the solution and the surface of the material.

Effect of Silicon Compounds

The inhibiting effect of silicon compounds was underlined clearly in the stress corrosion tests. Under all the conditions tested, the material showed greater resistance when compared to its behavior in NaOH. Characteristics of the polarization curves, with a wider passivation range and higher dissolution and passivation current densities, suggested a higher protective capacity for oxide layers formed in solutions containing silicon compounds. The AES performed on the deposits of the specimens confirmed that the silicon was incorporated into the oxide layers and that the Ni/Cr ratio was higher than in the base material, this agreeing with gradual dissolution of the material as discussed in the case of the reference specimens. The information obtained from this work was not sufficient to allow the determination of whether the better behavior observed in the solutions containing silicon compounds was caused by the incorporation of silicon in the oxide layer, making the latter more protective or simply that it had a barrier effect, preventing contact between the solution and the surface of the material. In addition, consideration might be given to a possible effect of the silicon compounds on the pH of the solutions, mitigating their aggressiveness.

Results appeared to disagree with the observations of other authors, who have carried out tests with small concentrations of SiO_2 at pH values close to neutral and in the presence of magnetite.[1,9-10] In the present work, the authors associated the presence of an alumino-silicate gel and the formation of a chromium-enriched layer, defined as nonprotective, with the greater aggressiveness of the environment. However, other authors indicate that when only SiO_2 is used, crack growth rate decreases by an order of magnitude compared to 10% NaOH, while the joint presence of SiO_2 and magnetite produces an increase in the rate of SCC.[22]

Results of the analyses performed on pulled tubes from operating plants indicated that the pres-
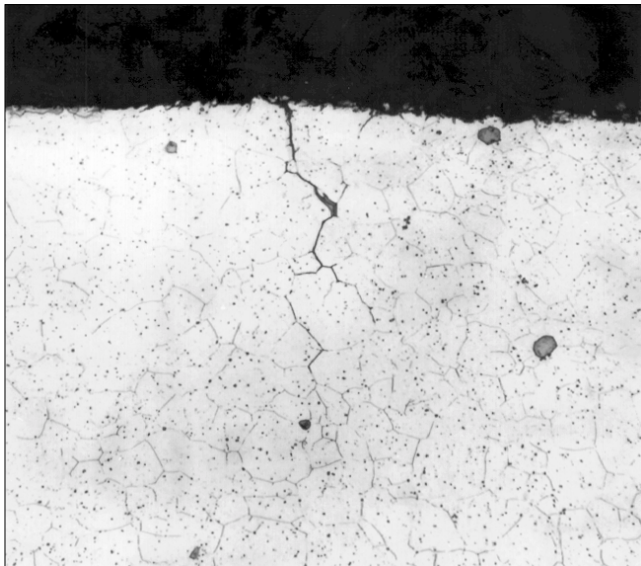
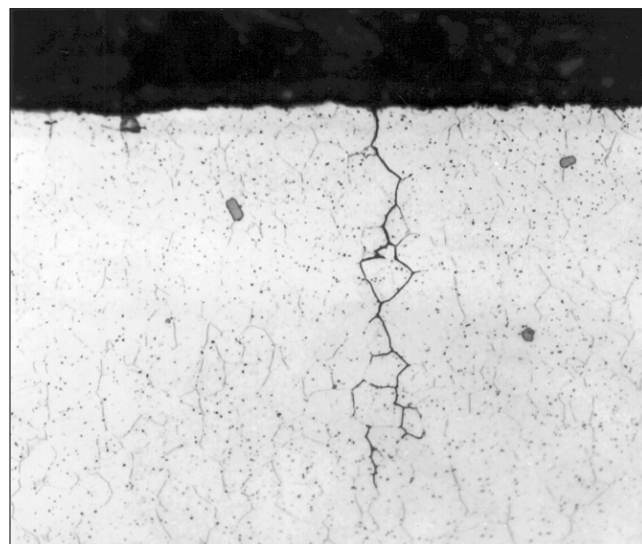FIGURE 13. *Detail of alloy 600MA tested in 7.5% SiO₂ + 10% NaOH, plus impurities at E_{act} during 1,000 h (500x).*
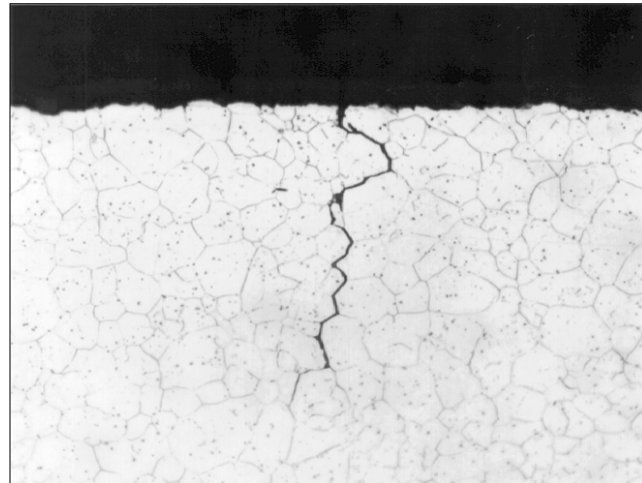
FIGURE 14. *Detail of alloy 600MA tested in 15% Na₂SiO₃ at E_{act} during 1,000 h (500x).*

FIGURE 15. *Detail of alloy 600MA tested in 15% Na₂SiO₃, plus impurities at E_{act} during 1,000 h (500x).*

ence of large quantities of silicon compounds is not associated always with the appearance of tube defects.[12,23] The molar ratio of Na/Cl in the blowdown has been used as a way of controlling IGA/SCC degradation processes in steam generator tubes, but not all operating plants obtain a good correlation between the defects observed and their chemistry when this ratio is considered. A recent study has shown that this correlation improves when other species are taken into account, such as SiO_2, calcium, and magnesium, and that the high concentration of SiO_2 in the blowdown is related to lower SCC in the tubes.[23]

Finally, the resistance of alloy 600MA in solutions with silicon compounds with and without impurities was similar. There was a slight improvement in the specimens tested at E_{act} since the cracks appeared over longer time periods. Other authors have shown that the damaging effect of certain impurities increased because of the presence of silicon.[6,22] However, taking into account that the impurities used were not harmful in the reference solution, this effect was not observed to increase in the solutions with silicon compounds. Furthermore, the presence of calcium and magnesium cations may have produced deposits containing insoluble silicates,[11] preventing contact between the surface of the metal and the solution, in keeping with the incorporation of magnesium in the oxide layer observed on the surfaces analyzed.

CONCLUSIONS

❖ Potentials applied in these tests did not have any effect on the IGA/SCC susceptibility of alloy 600MA in the long-term tests performed in caustic environments, in spite of the different oxide layers found on specimens tested at anodic potentials in 10% NaOH.

❖ An inhibiting effect was obtained with the silicon compounds (SiO₂ and Na₂SiO₃) on the IGA/SCC behavior of alloy 600MA in all of the solutions. This effect was suggested by the shape of the polarization curves and shown clearly by results of potentiostatic stress corrosion tests.

❖ The inhibiting effect of silicon compounds seemed to be related to the different layers formed on the specimen surfaces. The Auger depth profiles showed the incorporation of silicon and sodium in the outer layers.

❖ Impurities added to the NaOH solutions were not deleterious to the IGA/SCC susceptibilities of the
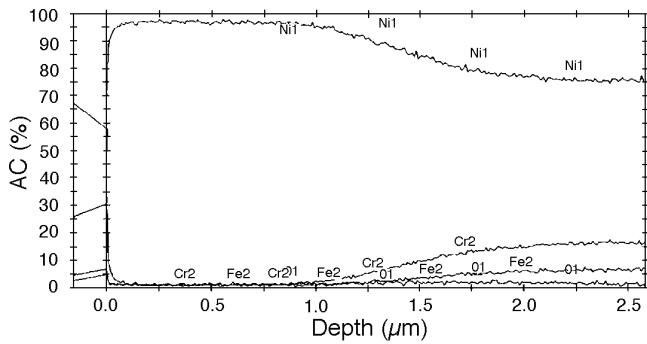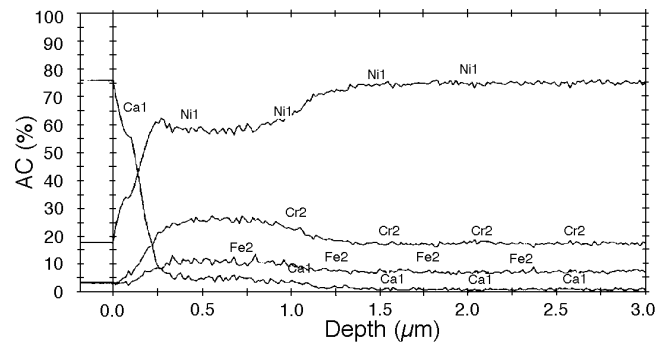
FIGURE 16. *AES depth profile at the outer diameter of alloy 600MA tested at E_{corr} during 750 h in 10% NaOH at 315°C (nickel, chromium, iron, and oxygen normalized to 100%).*
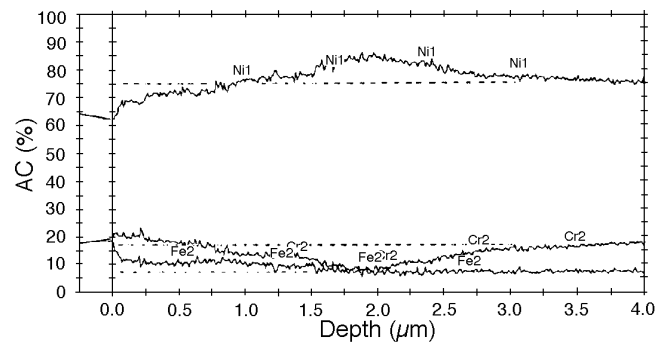
FIGURE 17. *AES depth profile at the outer diameter of alloy 600 MA tested at E_{act} during 250 h in 10% NaOH at 315°C (nickel, chromium, and iron normalized to 100%).*
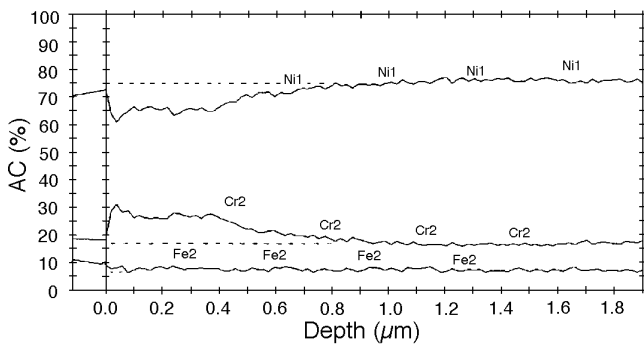
FIGURE 18. *AES depth profile at the outer diameter of alloy 600MA tested at E_{pass} during 250 h in 10% NaOH at 315°C (nickel, chromium, and iron normalized to 100%).*

FIGURE 19. *AES depth profile at the outer diameter of alloy 600MA tested at E_{pass} during 250 h in 10% NaOH plus impurities at 315°C (nickel, chromium, iron, and calcium normalized to 100%).*

alloys. In the case of silicon environments, they appeared to improve resistance to IGA/SCC, probably caused by the formation of insoluble silicates of calcium or magnesium.

ACKNOWLEDGMENTS

REFERENCES

1. B. Sala, P. Combrade, R. Erre, A. Gelpi, "Local Chemistry and Formation of Deposits on the Secondary Side of Steam Generators. A Laboratory Study," 6th Int. Symp. Environmental Degradation of Materials in Nuclear Power Systems — Water Reactors (Warrendale, PA: The Mineral, Metals, and Materials Society, 1993), p. 215.
2. G. Pinard-Legry, G. Plante, "Intergranular Attack of Alloy 600: High-Temperature Electrochemical Tests," EPRI NP-3062 (Palo Alto, CA: EPRI, 1983).
3. R. Bandy, D. Van Rooyen, "Intergranular Attack and Stress Corrosion Cracking of Alloy 600 in High-Temperature Caustic Solutions Containing Contaminants," EPRI NP-4051 (Palo Alto, CA: EPRI, 1987).
4. O. Cayla, P. Combrade, G. Slama, "About Some Possible Causes of IGA of Alloy 600 Tubes in Hot Caustic Solutions," 2nd Int. Symp. Environmental Degradation of Materials in Nuclear Power System — Water Reactors (La Grange Park, IL: American Nuclear Society, 1985).
5. R. Bergen, "Sodium Silicates — Stress Corrosion Cracking Agents for Alloys 600 and 690 at 3,150°C," Corrosion 41 (1985): p. 85.
6. W.M. Conner, R.G. Aspden, R. Hermer, N. Pessall, "Neutralization of Tubesheet Crevice Corrosion," EPRI NP-3040 (Palo Alto, CA: EPRI, 1983).
7. F.W. Pement, I.L. Wilson, R.G. Aspden, "Stress Corrosion Studies of High-Nickel Austenitic Alloys in Several High-Temperature Aqueous Solutions," MP (1980): p. 43-49.
8. G.P. Airey, "Optimization of Metallurgical Variables to Improve Corrosion Resistance of Inconel Alloy 600," EPRI NP-3051 (Palo Alto, CA: EPRI, 1983).
9. B. Sala, M. Organista, K. Henry, R. Errre, A. Gelpi, F. Cattant, M. Dupin, "Laboratory Study of Corrosion of Steam Generator Tubes: Preliminary Results," 7th Int. Symp. Environmental Degradation of Materials in Nuclear Power Systems — Water Reactors (Houston, TX: NACE, 1995), p. 259.
10. B. Sala, P. Combrade, A. Gelpi, K. Henry, R. Errre, A.M. Lancha, M. Dupin, "Analysis of the Deposits and Surface Layers on Tubes Pulled from PWR French Steam Generators," Eurocorr 96 (1996).
11. F. Catttant, M. Dupin, B. Sala, A. Gelpi, "Analyses of Depostis and Underlying Surfaces on the Secondary Side of Pulled Out Tubes from a French Plant," Int. Symp. Fonteuvrad III (1994), p. 469.
12. A.M. Lancha, D. Gómez-Briceño, M. García, C. Maffiotte, "Characterization of Ringhals 3 TSP Crevice and Tube Deposits," 8th Int. Symp. Environmental Degradation of Materials in Nuclear Power Systems — Water Reactors (La Grange Park, IL: American Nuclear Society, 1997).
13. J.J. Rowe, R.O. Fournier, G.W. Morey, "The System Water-Sodium-Oxide-Silicon Dioxide at 200, 250, and 3,000," Inorg. Chem. 6 (1967): p. 1,183.
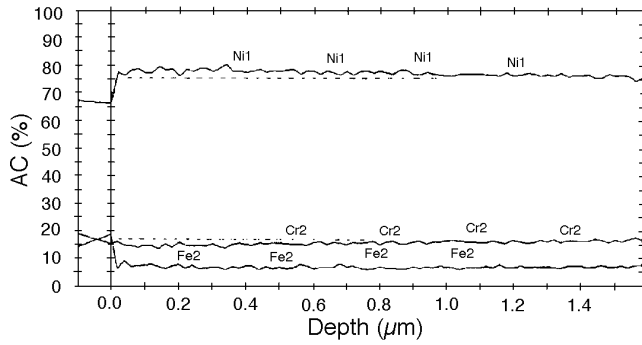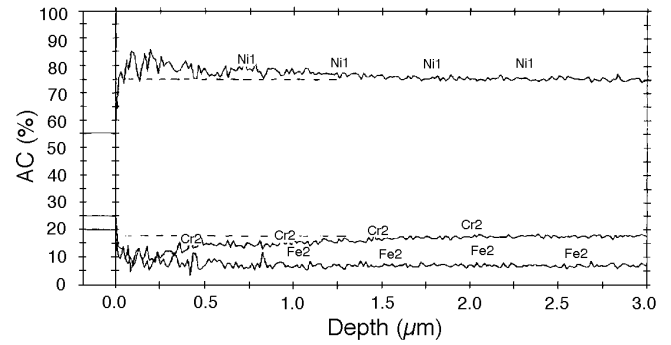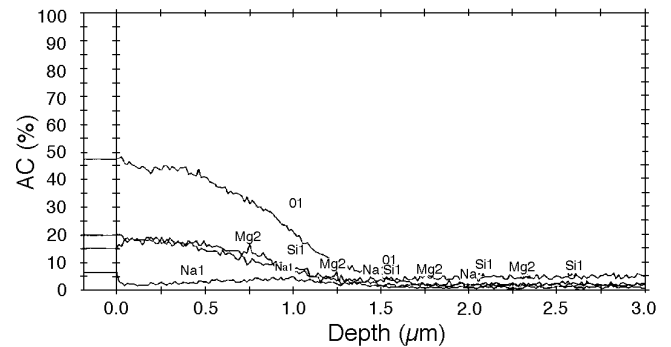
(a)
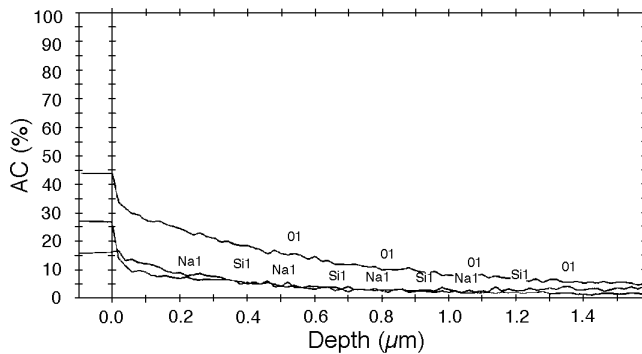
(b)

FIGURE 20. *AES depth profile at the outer diameter of alloy 600MA tested at E_{pass} during 1,000 h in 15% Na_2SiO_3 at 315°C: (a) nickel, chromium, and iron normalized to 100% and (b) nickel, chromium, iron, oxygen, sodium, and silicon normalized to 100%, although only sodium, silicon, and oxygen were represented.*

(a)

(b)

FIGURE 21. *AES depth profile at the outer diameter of alloy 600MA tested at E_{pass} during 1,000 h in 15% Na_2SiO_3, plus impurities at 315°C: (a) nickel, chromium, and iron normalized to 100% and (b) nickel, chromium, iron, oxygen, sodium, magnesium, and silicon normalized to 100%, although only sodium, magnesium, silicon, and oxygen were represented.*

14. N. Pesall, "Prediction of Stress Corrosion Cracking in 10% Caustic Soda Solutions at 3,150°C," Corros. Sci. 20 (1980): p. 225.
15. J.R. Cels, "Stress Corrosion Cracking of Stainless Steel and Nickel Alloys at Controlled Potentials in 10% Caustic Soda Solutions at 5,500°F," J. Electrochem. Soc. 123 (1976): p. 1,154.
16. J.B. Lumsden, "Inhibitors for IGA/IGSCC in Alloy 600 Steam Generator Tubes," Topical report EPRI (Palo Alto, CA: EPRI, 1993).
17. D. Van Rooyen, R. Bandy, "Mechanisms of Intergranular Attack and Stress Corrosion Cracking of Alloy 600 by High-Tempera-ture Caustic Solutions Containing Impurities," EPRI NP-5129 (Palo Alto, CA: EPRI, 1987).
18. P. Combrade, O. Cayla, M. Foucalt, D. Vancon, A. Gelpi, G. Slama, "About the Role of Surface Films on Alloy 600 Corrosion in High-Temperature Deaerated Environments," 3rd Int. Symp. Environmental Degradation of Materials in Nuclear Power Sys-tems — Water Reactors (Warrendale, PA: TMS, 1988), p. 525.

19. R.B. Rebak, Z. Sklarska-Smialowska, "Effect of Partial Pressure of Hydrogen on IGSCC of Alloy 600 in PWR Primary Water," Corrosion 47 (1991): p. 754.
20. B. Beverskog, I. Puigdomenech, "Revised Pourbaix Diagrams for Chromium at 25-3,000°C," Corros. Sci. 39 (1997): p. 43.
21. J.R. Bavalage, "Effect of Calcium Hydroxide and Carbonates on IGA and SCC of Alloy 600," EPRI NP-3060 (Palo Alto, CA: EPRI, 1983).
22. M.T. Miglin, J.V. Monter, C.S. Wade, M.J. Psaila, A.R. McIlree, "SCC of Alloy 600 in Complex Caustic Environments," 7th Int. Symp. Environmental Degradation of Materials in Nuclear Power Systems — Water Reactors (Houston, TX: NACE, 1995), p. 277.
23. A.J. Baum, P.J. Prabhu, M. Rootham, N.L. Zupetic, "Develop-ment of Improved PWR Secondary Water Chemistry Guidelines," 8th Int. Symp. Environmental Degradation of Materials in Nuclear Power Systems — Water Reactors (Grange Park, IL: American Nuclear Society, 1997).